Sensors & Transducers, Vol. 220, Issue 2, February 2018, pp. 37-44

www.sensorsportal.com

Sensors & Transducers

Published by IFSA Publishing, S. L., 2018
http://www.sensorsportal.com

Characterization of Cuprous Oxide Thin Films Prepared by Reactive Direct Current Magnetron Sputtering

[1, *] Ørnulf NORDSETH, [2] Irinela CHILIBON, [3] Raj KUMAR, [3] Kristin BERGUM, [2] Cristina VASILIU, [2] Raluca IORDANESCU, [2] Laurentiu BASCHIR, [2] Dan SAVASTRU, [2] Adrian KISS, [2] Anca PARAU, [4] Laurentiu FARA, [5] Roxana TRUSCA, [3] Edouard MONAKHOV, [1] Sean Erik FOSS and [3] Bengt Gunnar SVENSSON

[1] Institute for Energy Technology (IFE), Instituttveien 18, NO-2007 Kjeller, Norway
[2] National Institute of R&D for Optoelectronics (INOE-2000),
P.O. Box MG-5, RO-077125 Bucharest-Magurele, Romania
[3] Department of Physics/Center for Materials Science and Nanotechnology (SMN),
University of Oslo, P.O. Box 1048, Blindern, NO-0316 Oslo, Norway
[4] University Politehnica of Bucharest, 313 Spl. Independentei, RO-060042 Bucharest, Romania
[5] METAV-CD, 31 C. A. Rossetti, RO-020011 Bucharest, Romania
[*] Tel.: +47 6380 6000, fax: +47 6921 2201
[*] E-mail: ornulf.nordseth@ife.no

Received: 10 November 2017 /Accepted: 5 February 2018 /Published: 28 February 2018

Abstract: In this work, cuprous oxide (Cu_2O) thin films were prepared on silicon and quartz substrates by reactive direct current magnetron sputtering. The morphological and structural properties of the sputter-deposited Cu_2O thin films were investigated by scanning electron microscopy, atomic force microscope, and X-ray diffraction, whereas the optical properties were determined by spectroscopic ellipsometry and ultraviolet–visible spectrophotometer measurements. Thin film characterization showed that the average grain size for 500 nm thick Cu_2O film increases from about 70 nm for the as-grown film to about 600 nm after annealing the film at 900 °C in vacuum. Moreover, the surface roughness increased after annealing, whereas the optical absorption was reduced after annealing, presumably as a result of increased grain size and less strained films. The optical band gap increased from E_g = 2.06 eV for the as-grown Cu_2O film to E_g = 2.19 eV after annealing. X-ray diffraction scans showed diffraction peaks of (111), (200), and (220) planes of Cu_2O for both the as-grown and annealed film. The film resistivity and hole mobility were respectively 200 Ohm·cm and 50 $cm^2/V·s$ for the annealed Cu_2O film, derived from Hall effect measurements.

Keywords: Cuprous oxide, Thin films, Magnetron sputtering, Morphology, Optical properties.

1. Introduction

The p-type semiconductor cuprous oxide (Cu_2O) has been intensively studied due to its high optical absorption coefficient and favorable carrier transport properties. These characteristics combined with its non-toxic nature and abundant availability make Cu_2O attractive for various thin film technologies, such as photoelectrochemical systems [1], solar cells [2-3], photodetectors [4], and transistors [5]. Often,

the quality of the thin film is a constraining factor for successful incorporation of Cu_2O in such device applications. Several methods can be used to prepare Cu_2O thin films, including magnetron sputtering [6], molecular beam epitaxy [7], chemical vapor deposition [8], electrodeposition [9], thermal evaporation [10], and thermal oxidation [2]. One of the main advantages of magnetron sputtering is that it provides good control of the stoichiometry of the Cu_2O film by varying the process parameters, such as substrate temperature, gas mass flows, and target power density, in order to obtain Cu-rich or O-rich phases [11]. In addition, the technique enables the synthesis of thin films with high uniformity at a relatively high growth rate.

In this work, reactive direct current magnetron sputtering has been utilized to deposit uniform Cu_2O thin films of several hundred nanometer thickness on silicon and quartz substrates [12]. We show that annealing the sputter-deposited Cu_2O films at 900°C in vacuum improves the quality of the films, i.e., the optical and electrical properties are enhanced, and that the annealing process does not cause a transition to the oxygen-rich Cu_xO phases ($x < 2$).

2. Experimental Details

2.1. Materials and Synthesis

Cu_2O thin films were deposited on 1 × 1 cm^2 quartz and polished n-type silicon substrates by a direct current magnetron sputtering system (Semicore Triaxis). The substrates were cleaned in piranha and rinsed in deionized water. Diluted HF acid was used to remove the native surface oxide layer on the silicon substrates. Subsequently, the substrates were dried with nitrogen and loaded into the deposition chamber. Cu_2O was deposited by reactive sputtering of a Cu target (99.999 %) in O_2/Ar (6/49 sccm) with a substrate temperature of 400 ºC. The power density was fixed at 2.2 W/cm^2. Prior to the magnetron sputtering deposition, the base pressure was below 3.0×10^{-7} Torr. The sample stage was rotated at a constant speed of 12 rpm during the deposition process. The Cu_2O thin films were deposited at two different thicknesses, i.e., ~ 200 nm and ~ 500 nm, with a deposition rate ~ 25 nm/min. As-grown Cu_2O films were annealed at 900 ºC for 3 minutes in vacuum (pressure ~0.1 Torr). Table 1 presents the six different sputter-deposited Cu_2O thin film samples that were prepared and analyzed in this work.

2.2. Characterization

In order to study the morphology of the Cu_2O thin films, the samples were investigated using a QUANTA INSPECT F 50 scanning electron microscope (SEM) equipped with an electron field emission gun with a resolution of 1.2 nm. In addition, the samples were analyzed using a Veeco Innova atomic force microscope (AFM), with a RTESPA Si doped probe. The scanning was made in tapping mode and the scanning speed was about 2.5 μm/s on a surface area of 10 × 10 μm^2. The AFM images had a resolution of 512 × 512 pixels. SPM Lab Analysis v.7.0 software was utilized for the image analysis. The thin film thickness and complex refractive index were determined by spectroscopic ellipsometry, using an UVISEL ellipsometer from HORIBA Jobin Yvon in the wavelength range from 190 to 2100 nm. A model fit to the measured ellipsometry parameters was made using DeltaPsi ver. 2.6 software. The optical band gap of the Cu_2O films was determined from ultraviolet–visible spectrophotometer measurements (Shimadzu SolidSpe-3700 DUV) in the wavelength range from 290 to 1500 nm. X-ray diffraction (XRD) analysis was carried out using a Bruker AXS D8 Discover unit (with CuKα X-rays) in order to determine the crystal structure in normal θ-2θ scanning mode. Fourier-transform infrared (FTIR) spectroscopy was carried out using a Perkin Elmer type Spectrum 100 spectrometer, with accessory UATR, in the wavenumber range 430 - 2000 cm^{-1} with spectral resolution 0.4 cm^{-1}. Room temperature Hall effect measurements (LakeShore 7604) were carried out using the van-der Pauw configuration.

Table 1. Sample label and corresponding preparation conditions for the sputter deposited Cu_2O thin films.

Sample label	Cu_2O thin film preparation conditions
1	Cu_2O (as-grown): deposited at 400 °C on n-type Si substrate, 200 nm thickness
2	Cu_2O (as-grown): deposited at 400 °C on n-type Si substrate, 500 nm thickness
3	Cu_2O (as-grown): deposited at 400 °C on quartz substrate, 200 nm thickness
4	Cu_2O (as-grown): deposited at 400 °C on quartz substrate, 500 nm thickness
5	Cu_2O (annealed): deposited at 400 °C on quartz substrate; 200 nm thickness, annealed at 900 °C for 3 min in vacuum
6	Cu_2O (annealed): deposited at 400 °C on quartz substrate, 500 nm thickness, annealed at 900 °C for 3 min in vacuum

3. Results and Discussion

3.1. Scanning Electron Microscopy

SEM images of Samples 1-6 are shown in Fig. 1 - Fig. 6, respectively. In each image, the size of randomly selected grains is indicated. For Cu_2O films of 200 nm thickness deposited on n-type Si (Sample 1) the average grain size is around 30 - 40 nm, whereas for Cu_2O films of thickness 500 nm deposited on n-type Si (Sample 2) the average grain size is around 60 - 70 nm.

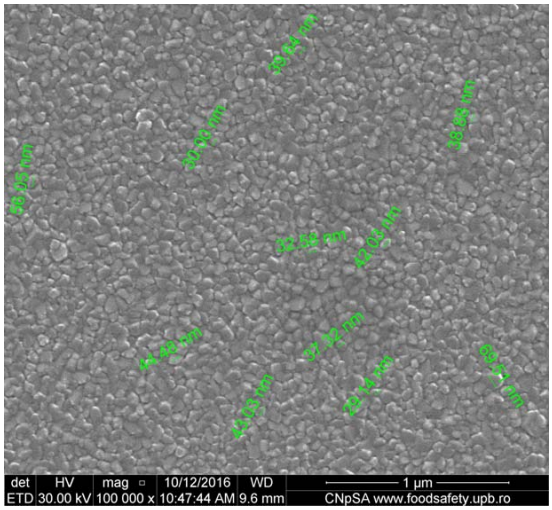

Fig. 1. SEM images of 200 nm as-grown Cu_2O thin film on Si substrate (Sample 1). The size of randomly selected grains is indicated in the image.

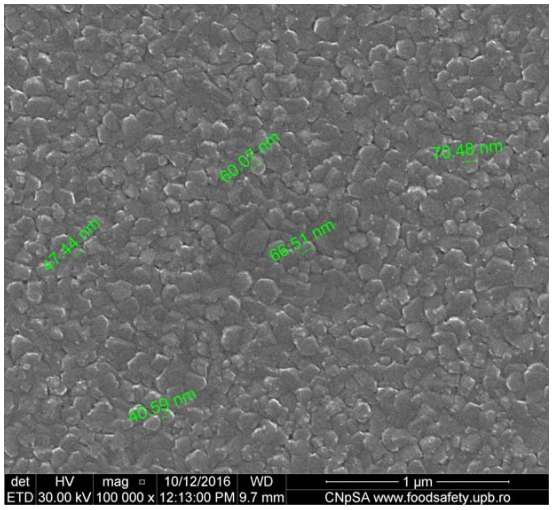

Fig. 2. SEM images of 500 nm as-grown Cu_2O thin film on Si substrate (Sample 2). The size of randomly selected grains is indicated in the image.

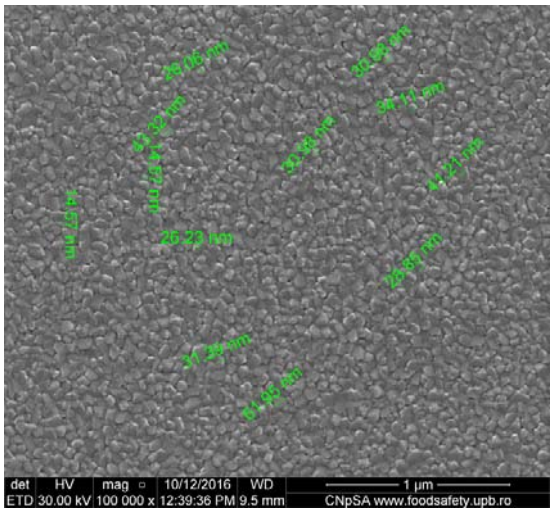

Fig. 3. SEM images of 200 nm as-grown Cu_2O thin film on quartz substrate (Sample 3). The size of randomly selected grains is indicated in the image.

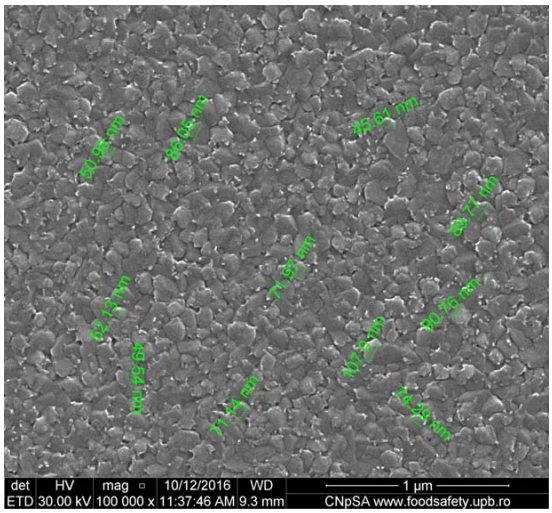

Fig. 4. SEM images of 500 nm as-grown Cu_2O thin film on quartz substrate (Sample 4). The size of randomly selected grains is indicated in the image.

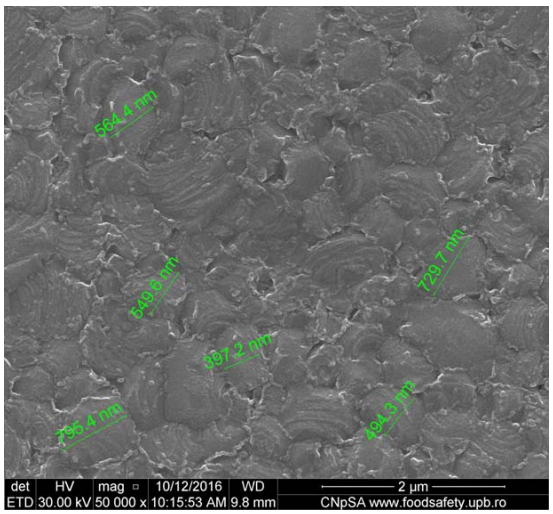

Fig. 5. SEM images of 200 nm annealed Cu_2O thin film on quartz substrate (Sample 5). The size of randomly selected grains is indicated in the image.

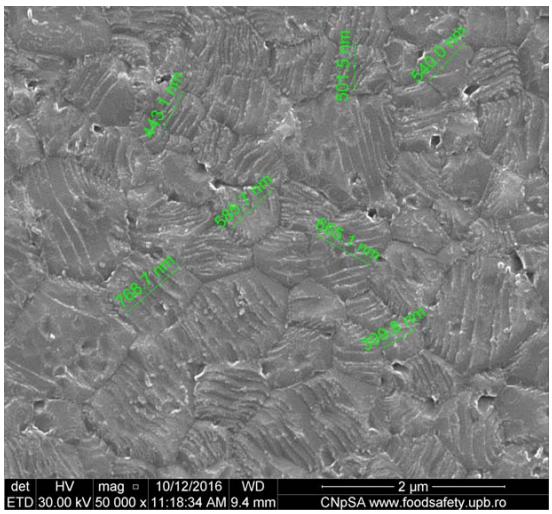

Fig. 6. SEM images of 500 nm annealed Cu_2O thin film on quartz substrate (Sample 6). The size of randomly selected grains is indicated in the image.

For Cu_2O films deposited on quartz substrate, increasing the film thickness from 200 nm (Sample 3) to 500 nm (Sample 4) results in a similar increase in the grain size as in the Samples 1 and 2. In general, based on the recorded SEM images there is no apparent difference in the morphology for films deposited on Si or quartz substrate.

The SEM images for the 200 nm (Sample 5) and 500 nm (Sample 6) annealed Cu_2O film deposited on quartz show that the average grain size increases to about 600 nm after annealing. In general, for thin-film optical applications it is desirable to have a columnar grain structure with a lateral grain size that is larger than the thickness of the thin film [13].

3.2. Atomic Force Microscopy

AFM images (10 μm × 10 μm) of Samples 2 - 6 are shown in Fig. 7 – Fig. 11, respectively. For Sample 1, an AFM image was not recorded.

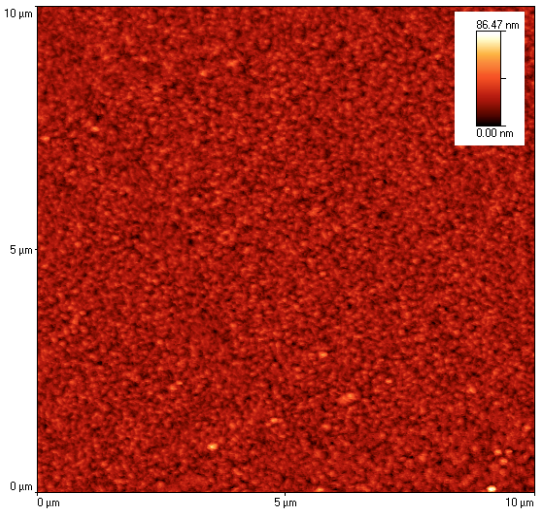

Fig. 7. AFM image of 500 nm as-grown Cu_2O film on Si substrate (Sample 2).

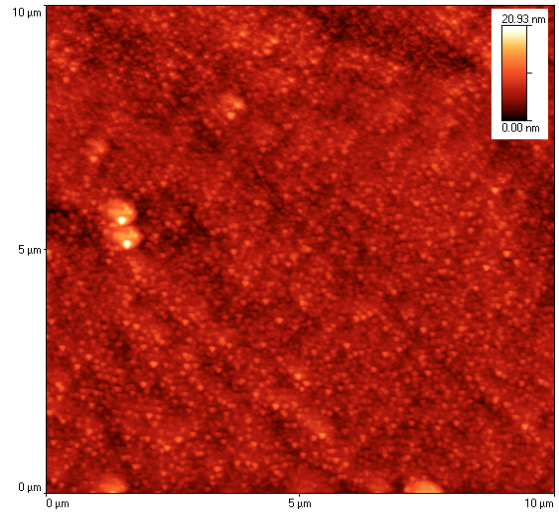

Fig. 8. AFM image of 200 nm as-grown Cu_2O film on quartz substrate (Sample 3).

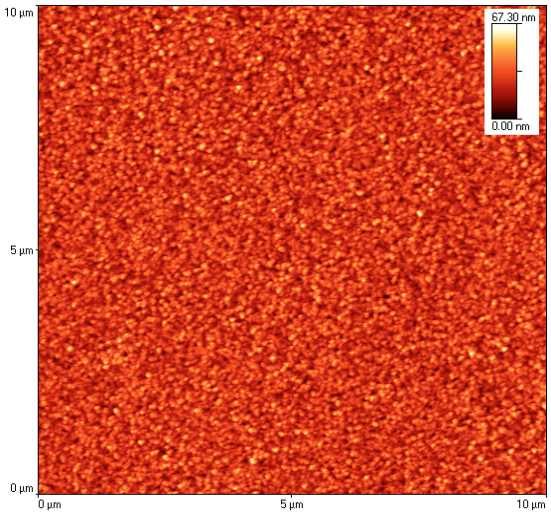

Fig. 9. AFM image of 500 nm as-grown Cu_2O film on quartz substrate (Sample 4).

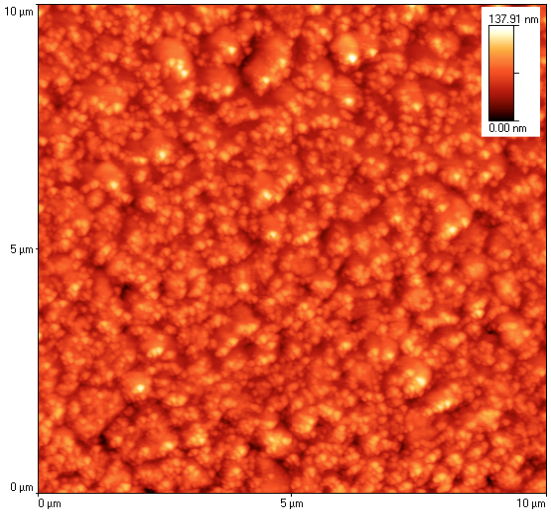

Fig. 10. AFM image of 200 nm annealed Cu_2O film on quartz substrate (Sample 5).

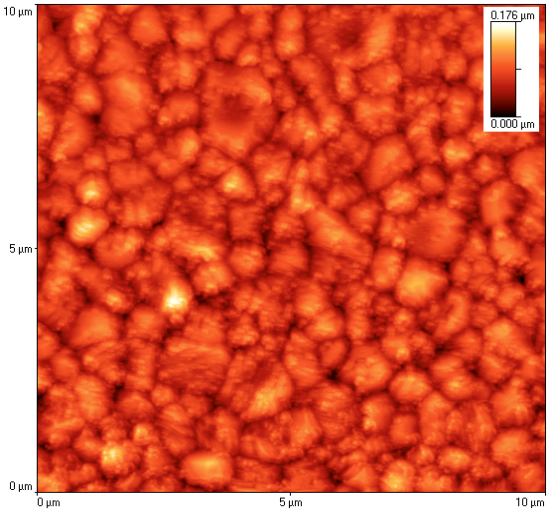

Fig. 11. AFM image of 500 nm annealed Cu_2O film on quartz substrate (Sample 6).

The root-mean square surface roughness (R_{RMS}) for each sample was extracted from the AFM images. R_{RMS} is defined as the standard deviation of the surface height profile from the mean height, given by

$$R_{RMS} = \left[\frac{1}{N} \sum_{n-1}^{n} \left(h_i - \langle h \rangle \right)^2 \right]^{\frac{1}{2}}, \quad (1)$$

where N is the number of pixels in the image (or data points), h_i is the height of the i^{th} pixel, and h is the mean height of the image [14]. In Table 2, the R_{RMS} is given for each sample. The data shows that an increase in the thickness of the Cu_2O films results in an increase of the surface roughness, and that R_{RMS} is comparable for films of same thickness deposited on Si and quartz, e.g., Sample 2 and 4 have similar surface roughness. Furthermore, the R_{RMS} for the Cu_2O films deposited on quartz increases after annealing at 900 °C for 3 minutes in vacuum, with Sample 6 having the largest R_{RMS} of about 21 nm.

Table 2. R_{RMS} for sputter deposited Cu_2O thin films. Sample 1 was not analyzed.

Sample label	R_{RMS} (nm)
1	N.A.
2	6.31
3	1.58
4	7.95
5	15.65
6	20.60

3.3. Optical Properties

For analysis of the measured spectroscopic ellipsometry parameters Ψ and Δ, a model consisting of a Cu_2O layer with a surface roughness layer and an interface layer on the substrate was adopted. The surface roughness was modeled by mixing the optical constants of the surface material (Cu_2O) and 50 % air. The complex refractive index for Cu_2O was modeled using a Tauc-Lorentz dispersion formula. In the calculations, the optical properties of each material in the respective layer were based on values reported in the literature. The recorded ellipsometry parameters were modeled until the best fit was obtained. Fig. 12 shows the calculated wavelength dispersion of the refractive index n and the extinction coefficient k for the as-grown (Sample 4) and annealed (Sample 6) Cu_2O thin film on quartz, as obtained from the numerical fit to spectroscopic ellipsometry data. The extracted wavelength dispersion for n and k corresponds well with the dispersion relations previously reported for Cu_2O films [15]. The ellipsometry data suggests that both n and k decrease in the wavelength region below ~450 nm after the vacuum annealing at 900 °C relative to those of the as-grown film.

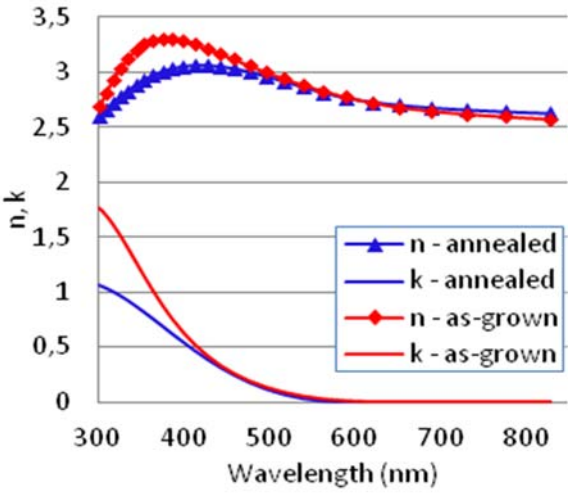

Fig. 12. Refractive index n and extinction coefficient k for the 500 nm as-grown (Sample 4) and annealed (Sample 6) Cu_2O film on quartz.

The optical transmittance spectra for the Cu_2O films (data not shown) suggest that the transmittance properties are enhanced in the visible and near-infrared wavelength range after annealing [3], which is likely due to the larger grain size (cf. Fig. 6) and a corresponding reduction of grain-boundary scattering [16], possibly together with less strained film. Based on the optical transmittance spectra for the 500 nm thick as-grown (Sample 4) and annealed (Sample 6) Cu_2O thin films on quartz, a Tauc plot analysis was carried out to determine the optical band gap [11]. Fig. 13 shows the resulting Tauc plots, suggesting that the optical band gap increases from E_g = 2.06 eV for the 500 nm as-grown Cu_2O film to E_g = 2.19 eV after annealing at 900°C. The widening of the optical band gap after annealing might be due to partial elimination of defects states [16] and possibly more phase-pure Cu_2O films.

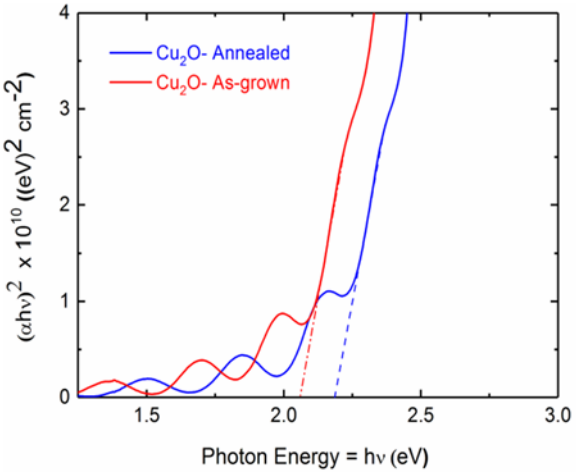

Fig. 13. Tauc plot for the 500 nm as-grown (Sample 4) and annealed (Sample 6) Cu_2O film on quartz. The optical band gap values are estimated from extrapolation to the abscissa (dashed lines).

3.4. X-ray Diffraction

Fig. 14 shows θ-2θ scans for the 500 nm thick as-grown (Sample 4) and annealed (Sample 6) Cu_2O films deposited on quartz in the 2θ range 30-65°. The XRD data suggests that there exist several crystalline orientations for both the as-grown and the annealed Cu_2O film, i.e., the diffraction peaks at ~36.5°, ~42.4°, ~61.8°, corresponding to reflection from the Cu_2O(111), Cu_2O(200), and Cu_2O(220) planes, respectively. After annealing at 900 °C, the (111) and (220) diffraction peaks become narrower, possibly indicating strain relaxation, whereas the (200) diffraction peak decreases in intensity. The θ-2θ scans also suggest that there is no presence of other Cu_xO phases, e.g., there are no diffraction peaks of the cupric oxide (CuO) and copper (III) oxide (Cu_4O_3) phases for both the as-grown and the annealed film.

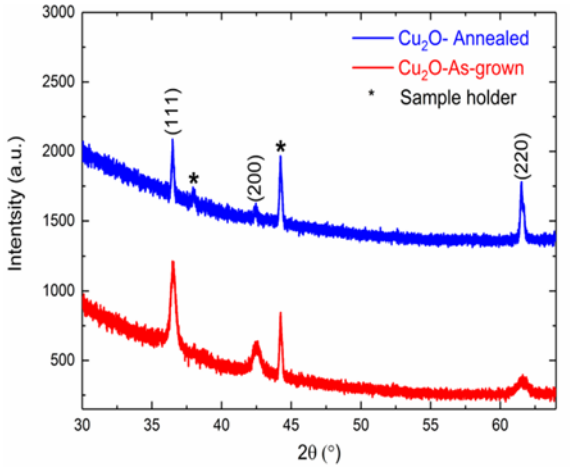

Fig. 14. θ-2θ scans for the 500 nm thick as-grown (Sample 4) and annealed (Sample 6) Cu_2O film on quartz.

3.5. Fourier-transform Infrared Spectroscopy

The FTIR transmission spectra for the 200 nm thick as-grown Cu_2O film deposited on Si (Sample 1) and 200 nm thick as-grown (Sample 3) and the annealed (Sample 5) Cu_2O films on quartz are shown in Fig. 15. The absorption peaks at wavenumber ~615 cm^{-1} and 645 cm^{-1} (indicated by dashed lines) are characteristic of Cu_2O and are observed for all three samples. The peak at wavenumber ~556 cm^{-1} (indicated by dashed line) is characteristic of CuO and is observed for the Cu_2O films deposited on quartz (Sample 3 and Sample 5). This could be explained by oxidation of Cu_2O, i.e., a small amount of Cu_2O at the interface with the quartz substrate is transformed into CuO. No peaks characteristic of CuO is observed for the Cu_2O film deposited on Si (Sample 1). Furthermore, there is no major difference between the recorded FTIR transmission spectra for the as-grown and annealed Cu_2O films deposited on quartz, which suggests that the film is stoichiometry-stable when heated to 900 °C at a pressure of 0.1 Torr, i.e., the annealing process does not cause a transition to the more oxygen-rich phases.

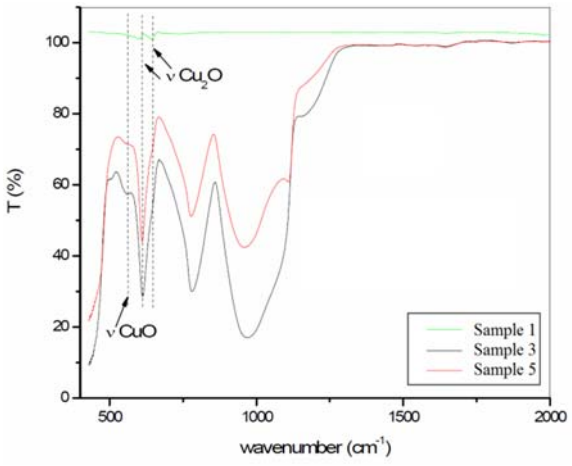

Fig. 15. FTIR transmission (T) vs. wavenumber for 200 nm Cu_2O films on Si and quartz. The Cu_2O absorption peaks at ~615 cm^{-1} and ~645 cm^{-1} and the CuO absorption peak at ~556 cm^{-1} are indicated by the dashed lines.

3.6. Electrical Properties

The Cu_2O films display p-type conductivity. The majority carrier (hole) mobility, film resistivity, and majority carrier concentration for 500 nm as-grown (Sample 4) and annealed (Sample 6) Cu_2O films on quartz, derived from room temperature Hall effect measurements, are presented in Table 3. The Hall measurements evidence that the electrical properties of the Cu_2O thin film are improved after the 900 °C annealing, i.e., the hole mobility increases from 10 to 50 $cm^2/V{\cdot}s$ and the resistivity decreases from 560 to 200 Ω·cm. These values are comparable to those reported previously for sputter-deposited polycrystalline Cu_2O thin films on quartz [6, 17]

Table 3. Majority carrier (hole) mobility, film resistivity, and majority carrier concentration for 500 nm as-grown (Sample 4) and annealed (Sample 6) Cu_2O films on quartz.

Property	Sample 4	Sample 6
Carrier mobility ($cm^2/V{\cdot}s$)	10	50
Resistivity (Ohm·cm)	560	200
Carrier concentration (cm^{-3})	3×10^{15}	1×10^{15}

7. Conclusions

High-quality Cu_2O thin films were synthesized by reactive direct current magnetron sputtering. Characterization by scanning electron microscopy and atomic force microscopy showed that the average

grain size and the surface roughness increase with film thickness. Spectroscopic ellipsometry measurements reveal that the optical absorption is reduced after annealing of the Cu_2O film at 900 °C, i.e. the extinction coefficient is reduced, presumably as a result of increased grain size. The widening of the optical band gap from E_g = 2.06 eV for the as-grown Cu_2O film to E_g = 2.19 eV after annealing, as observed from Tauc plots, might be due to partial elimination of defects states and strain relaxation. XRD and FTIR spectroscopy measurements suggest that the Cu_2O films are stoichiometry-stable when annealed at 900 °C and a pressure of 0.1 Torr. Hall effect measurements show that the electrical properties of the Cu_2O film are improved after annealing, resulting in a high carrier mobility (50 $cm^2/V{\cdot}s$) and low resistivity (200 Ohm·cm).

In conclusion, the thin film characterization carried out in this work suggests that the optical and electrical properties of the sputter-deposited Cu_2O films are improved after the annealing at 900 °C and that the high-temperature annealing process does not cause a transformation to the more oxygen-rich Cu_xO phases ($x < 2$). Potential applications for the p-type Cu_2O films include all-oxide based p-n heterojunction devices, such as p-Cu_2O/n-ZnO photodetectors [4] and solar cells [18].

Acknowledgements

This work was conducted under the research project “High-performance tandem heterojunction solar cells for specific applications” (SOLHET), project number 251789, financially supported by the Research Council of Norway (RCN) and the Romanian Executive Agency for Higher Education, Research, Development and Innovation Funding (UEFISCDI) through the M-ERA.NET European Program and 2017 Core Program, PN16-400102.

References

[1]. H. Qi, J. Wolfe, D. Fichou, Z. Chen, Cu_2O Photocathode for Low Bias Photoelectrochemical Water Splitting Enabled by NiFe-Layered Double Hydroxide Co-Catalyst, *Scientific Reports*, Vol. 6, 2016, 30882.

[2]. T. Minami, Y. Nishi, T. Miyata, Efficiency enhancement using a Zn_{1-x} Ge_x -O thin film as an n-type window layer in Cu_2O-based heterojunction solar cells, *Applied Physics Express*, Vol. 9, Issue 5, 2016, 052301.

[3]. Ø. Nordseth, R. Kumar, K. Bergum, L. Fara, S. E. Foss, H. Haug, F. Dragan, D., Crăciunescu, P. Sterian, I. Chilibon, C. Vasiliu, L. Baschir, D. Savastru, E. Monakhov, B. G. Svensson, Optical analysis of a ZnO/Cu_2O subcell in a silicon-based tandem heterojunction solar cell, *Green and Sustainable Chemistry*, Vol. 7, No. 1, 2017, pp. 57-69.

[4]. Y. H. Ok, K. R. Lee, B. O. Jung, Y. H. Kwon, H. K. Cho, All oxide ultraviolet photodetectors based on a p-Cu_2O film/n-ZnO heterostructure nanowires, *Thin Solid Films*, Vol. 570, 2014, pp. 282-287.

[5]. K. Matsuzaki, K. Nomura, H. Yanagi, T. Kamiya, M. Hirano, H. Hosono, Epitaxial growth of high mobility Cu_2O thin films and application to p-channel thin film transistor, *Applied Physics Letters*, Vol. 93, Issue 20, 2008, pp. 202107-202107-3.

[6]. S. Ishizuka, T. Maruyama, K. Akimoto, Thin-film deposition of Cu_2O by reactive radio-frequency magnetron sputtering, *Japanese Journal of Applied Physics*, Vol. 39, Issue Part 2, No. 8A, 2000, pp. L786-L788.

[7]. D. S. Darvish, H. A. Atwater, Epitaxial growth of Cu_2O and ZnO/Cu_2O thin films on MgO by plasma-assisted molecular beam epitaxy, *Journal of Crystal Growth*, Vol. 319, 201, pp. 39-43.

[8]. S. H. Jeong, E. S. Aydil, Structural and electrical properties of Cu_2O thin films deposited on ZnO by metal organic chemical vapor deposition, *Journal of Vacuum Science & Technology A: Vacuum, Surfaces, and Films*, Vol. 28, Issue 6, 2010, pp. 1338-1343.

[9]. W. Zhao, W. Fu, H. Yang, C. Tian, M. Li, Y. Li, L. Zhang, Y. Sui, X. Zhou, H. Chen, G. Zou, Electrodeposition of Cu_2O films and their photoelectrochemical properties, *CrystEngComm*, Vol. 13, 2011, pp. 2871-2877.

[10]. M. F. Al-Kuhaili, Characterization of copper oxide thin films deposited by the thermal evaporation of cuprous oxide (Cu_2O), *Vacuum*, Vol. 82, Issue 6, 2008, pp. 623-629.

[11]. J. Gan, V. Venkatachalapathy, B.G. Svensson, E. V. Monakhov, Influence of Target Power on Properties of Cu_xO Thin Films Prepared by Reactive Radio Frequency Magnetron Sputtering, *Thin Solid Films*, Vol. 594, 2015, pp. 250-255.

[12]. Ø. Nordseth, B. G. Svensson, R. Kumar, I. Chilibon, S. E. Foss, C. Vasiliu, R. Iordanescu, L. Baschir, D. Savastru, L. Fara, A. Kiss, A. Parau, Cu_2O Photosensitive Thin Films for Solar Cell Application, in *Proceedings of the Eighth International Conference on Sensor Device Technologies and Applications*, Rome, Italy, 10-14 September 2017, pp. 47-52.

[13]. M. Imaizumi, T. Ito, M. Yamaguchi, K. Kaneko, Effect of Grain Size and Dislocation Density on the Performance of Thin Film Polycrystalline Silicon Solar Cells, *Journal of Applied Physics*, Vol. 81, Issue 11, 1997, pp. 7635-7640.

[14]. J. M. Bennett, L. Mattson, Introduction to Surface Roughness and Scattering, *Optical Society of America*, Washington, DC, 1989.

[15]. C. Malerba, F. Biccari, C. L. A. Ricardo, M. D’Incau, P. Scardi, A. Mittiga, Absorption Coefficient of Bulk and Thin Film Cu_2O, *Solar Energy Materials and Solar Cells,* Vol. 95, Issue 10, 2011, pp. 2848-2854.

[16]. Y. Wang, P. Miska, D. Pilloud, D. Horwat, F. Mücklich, J. F. Pierson, Transmittance enhancement and optical band gap widening of Cu_2O thin films after air annealing, *Journal of Applied Physics*, Vol. 115, 2014, 073505.

[17]. Y. S. Lee, M. T. Winkler, S. C. Siah, R. Brandt, T. Buonassisi, Hall mobility of cuprous oxide thin films deposited by reactive direct-current magnetron sputtering, *Applied Physics Letters*, Vol. 98, Issue 19, 2011, pp. 1-3, 192115.

[18]. Ø. Nordseth, L. Fara, R. Kumar, S. E. Foss, C. Dumitru, V.-F. Muscurel, F. Drăgan, D. Crăciunescu, K. Bergum, H. Haug, P. Sterian, I. Chilibon, C. Vasiliu, L. Baschir, D. Savastru, E. Monakhov, B. G. Svensson, Electro-optical modeling of a ZnO/Cu_2O subcell in a silicon-based tandem heterojunction solar cell, in *Proceedings of the 33rd European Photovoltaic Solar Energy Conference and Exhibition,* Amsterdam, The Netherlands, 25-29 September 2017, pp. 172-177.